



Sharif University of Technology

Scientia Iranica

Transactions A: Civil Engineering

<http://scientiairanica.sharif.edu>

Failure analysis of the 16-story Plasco building under fire condition

S. Epackachi^{a,*}, S.R. Mirghaderi^b, and P. Aghelizadeh^a

a. Department of Civil and Environmental Engineering, Amirkabir University of Technology, Tehran, Iran.

b. School of Civil Engineering, College of Engineering, University of Tehran, Tehran, Iran.

Received 24 March 2021; received in revised form 20 August 2021; accepted 3 January 2022

KEYWORDS

Progressive collapse;
Plasco steel building;
Nonlinear finite
element analysis;
Fire effects;
Design
recommendation.

Abstract. The progressive collapse of the 16-story Plasco steel building induced by fire in Tehran on 19 January 2017 led to the death of dozens of firefighters. This paper presents the results of a comprehensive 3D nonlinear finite element analysis for a floor of the Plasco building under fire condition. The LS-DYNA program is used to investigate the cause of steel beam-to-column connection failure. Results of the nonlinear analysis of detailed numerical model confirm the failure modes of the structural elements such as columns, trusses, joists, beams, welds, and other structural elements investigated during the site visits. Design recommendations are provided based on the results from the fire analysis of the Plasco building.

© 2022 Sharif University of Technology. All rights reserved.

1. Introduction and background

The 16-story Plasco building, as an important commercial center in Tehran, experienced an accidental fire that led to the collapse of the entire building. There are such similar fire-induced incidents like World Trade Center 5 [1], Alexis Nilton Plaza [2], and One New York Plaza [3]. Inspection reports from these fire incidents indicate that the failure of the steel connections was reported to be the main source of its collapse in most cases. Therefore, extensive researches have been conducted to investigate the response of steel connections subjected to fire over the past few decades. In the following, a summary of the numerical and

experimental studies on common welded and bolted steel connections is provided.

Rahnavard et al. [4] conducted a numerical study on three types of rigid connections, namely flush end-plate, connection with bolted cover plate, and bolted T joint at elevated temperatures using the ABAQUS software. The numerical models were validated using data from tests conducted by Wald et al. [5] through the elastic and plastic ranges up to failure. Based on the results of numerical analysis, out of three connections, the end-plate connection had a better performance with lower stiffness degradation and lateral buckling. Eslami et al. [6] developed a finite element model to predict the behavior of bolted splice connections under fire condition. Three major types of nonlinearities including geometric, material, and contact nonlinearities were considered. Parametric studies were conducted using the validated proposed model. The above study demonstrated that the free length of flange splice plate and thermal gradients affected the fire behavior of the connections significantly. Sarraj et al. [7] studied the robustness of fin plate connections under catenary

*. Corresponding author. Tel.: +98 21 64543007
E-mail addresses: epackachis@aut.ac.ir. (S. Epackachi);
rmirghaderi@ut.ac.ir. (S.R. Mirghaderi);
aghelizadehpariya@gmail.com. (P. Aghelizadeh)

action in fire using nonlinear finite element models incorporating geometric and material nonlinearities as well as contact behavior. The developed models predicted the behavior of specimens tested by Wald et al. [8] with bolt shear as the predominant failure mode. Al-Jabri et al. [9] conducted a numerical study on four elevated-temperature models to investigate the behavior of flush end-plate connections. The ABAQUS predicted response was compared to the data obtained from tests conducted by Al-Jabri et al. [10]. The numerical results including failure modes and moment-rotation curves of the connection exhibited reasonable agreement with experimental results. Daryan and Yahyai [11] investigated the behavior of bolted angle connections subjected to concentrated forces at elevated temperatures with and without web angles using ten nonlinear finite element models. A series of tests including two different types of connections, namely specimens without web angle and specimens with web angle, conducted by Daryan [12] and Daryan and Yahyai [13] were employed to validate the proposed model. The failure modes and moment-rotation curves agreed with the experimental results.

Zhu and Li [14] tested five welded connections under heating and natural cooling process. H-section beam and H-section column flanges were connected with all-through butt welds. The beam web and column flange were connected with double-sided fillet welds. Results showed that the failure mode of connections changes from beam flange buckling in the ambient temperature to the butt weld cracking at elevated temperatures. Zhang et al. [15] tested three common types of welded connections, namely butt-welded, transverse, and longitudinal fillet welded connections, subjected to high temperatures and cooling. For each type of connection, 39 specimens with high-strength steel were constructed. The above study illustrated that the transverse and longitudinal fillet welded connection specimens experienced failure in the base metal and the other specimens failed in the butt-welded connections. Guo and Huang [16] conducted a numerical study on Reduced Beam Section (RBS) connections under fire condition using the finite element ABAQUS software. Results of RBS connections were compared to those of typical steel beam with fin-plate connections. The comparison showed that the flanges were cut in the RBS beams, providing rotational and axial ductility to the connections that led to higher fire resistance than those of typical beams. Seif et al. [17] performed a numerical study on the fire performance of steel moment frames with welded unreinforced flange, bolted web (WUF-B) connections, and RBS connections using the LS-DYNA program. Material with temperature-dependent properties for structural steel and bolts were considered for both models. In addition, the fracture of the elements of bolted web (WUF-B)

assembly was considered using an erosion criterion. Results showed that local buckling caused the failure of both WUF-B and RBS connections during the heating phase.

Fletcher et al. [18] provided a “state-of-the-art” review of research on the effects of temperature on concrete and concrete structures. This review demonstrated that the response of concrete subjected to fire was complex depending on its mix properties, maximum fire temperature, and fire duration. This local complexity together with issues of fire analysis of the whole structure led to significant challenges for fire analysis of concrete structures. Jiang and Usmani [19] examined the accuracy of the thermo-mechanical analysis of steel structures developed in OpenSees using the test data and results of finite element analysis for beams and frame structures subjected to fire. This research indicated that the constitute model in OpenSees for fire analysis could predict the thermal responses for various ranges of steel structures successfully. The response of World Trade Center (WTC) tower to fire along with various collapse scenarios was investigated by Kotsovinos and Usmani [20]. They identified two collapse mechanisms including weak and strong floor mechanisms by analyzing a simple and typical composite frame structure subjected to fire. The same failure mechanisms of tall building in fire were proposed by Lange et al. [21]. A simple fire assessment methodology was proposed.

Although the previous study by the authors [22] investigated the major sources of fire initiation and collapse of the Plasco building, the fire performance of connections that failed during the fire has not been studied yet. Herein, the results of the detailed numerical analysis of a part of the Plasco building including columns, girders, joists, slab, and connections subjected to gravity and thermal loads are presented and discussed. The failure modes of the connections and other structural components resulting in total collapse of the structure are also presented. Based on the analysis results, design recommendations are provided.

2. Specifications of the Plasco building

2.1. The structure of the building

The Plasco building was a 16-story building including a basement, a ground floor, and fourteen stories above the ground. The elevation view of the building is presented in Figure 1. The typical numbering of the building is shown on the right side of the figure.

The structural plan view of the building is shown in Figure 2. Except the basement, all other stories were constructed using steel members.

As shown in Figure 3, the flooring system con-

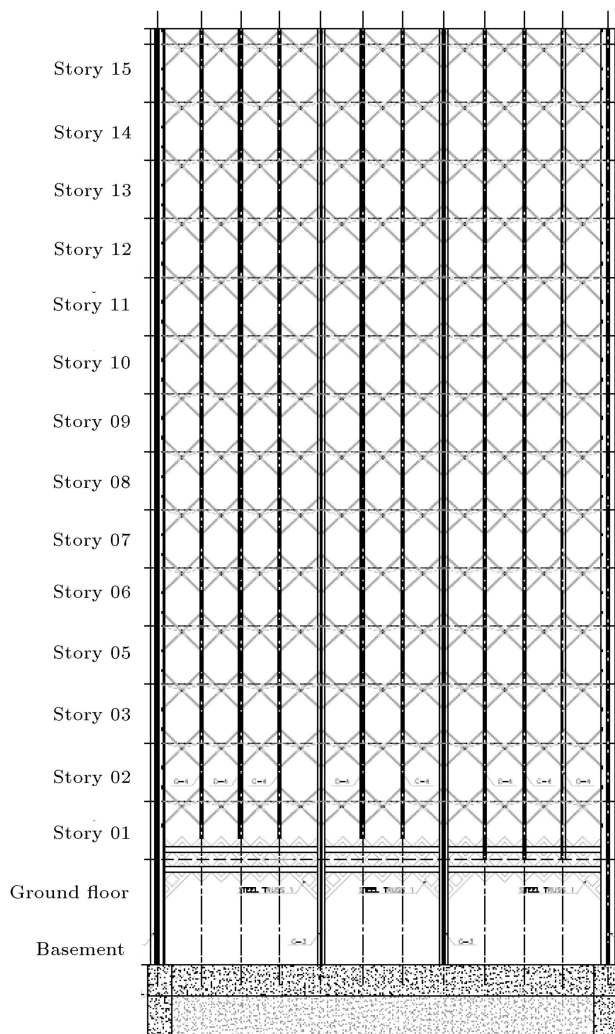


Figure 1. Elevation view of the Plasco building.

sisted of a 130 mm thickness concrete slab with 150 mm spaced steel reinforcement. The joists and tie beams were designed to support the concrete floor slab.

A tube frame system including closely spaced columns and short span beams with diagonal braces in the perimeter of the structure was used as a lateral force-resisting system for the Plasco building. A concrete slab with four large columns and truss girders and a number of joists was used as the gravity system. All of the structural members were made using built-up sections. The corner columns were made using four double channels connected using steel box members. The perimeter columns, located on the main axis of the building, were made using two double channels, while other perimeter columns were made using just one double channel. The interior columns were made using four double channels. The cross-section views of the corner, perimeter, and interior columns are shown in Figure 4.

The joists and girders used in the Plasco building are shown in Figures 5–7. The top and bottom chords

of the joists were made using double angles. The web of the joists consisted of diagonal double bars and vertical plates. The configuration of the girders was similar to that of the joists, except that the bottom chords were made using double channels and diagonal plates in joists.

The dead and live loads, considered in the analysis, are 550 kg/m^2 and 100 kg/m^2 , respectively. The dead load includes the weight of the ceiling, concrete slab, flooring, partition, and mechanical equipment. The weight of the structural components is automatically computed in the analysis.

3. Numerical analysis of the Plasco building

The general-purpose finite element code, LS-DYNA [23,24], is used to simulate the nonlinear and collapse behavior of two-quarters of the most critical panel of a typical floor. The modeled zones are presented in Figure 8.

The models included the half-length of the columns above and below the floor, the half-length of the girders, joists, and ties, a quarter of the slab and its reinforcement, the connections between the girder and column, joist and girder, and tie and joists, as presented in Figures 9 and 10. Both geometrical and material nonlinearities were considered in numerical analysis.

The boundary conditions at the edges of the two-modeled panels are presented in Figure 11. The three numbers from left to right in each edge panel indicate the restraint condition along x , y , and z axes, respectively, where the x - y plane is parallel to concrete slab. The fixed and free translational motions along x , y , or z axes are denoted by 1 and 0, respectively.

The slab reinforcement is tied to the concrete elements. The available contact algorithms in the software are used to consider friction between the concrete slab and the steel girders and joists and to avoid penetration of the adjacent steel elements. Except for the slab reinforcement, all other elements including the steel column, girder, joist, tie, connections, and concrete slab are modeled using an eight-node solid element with a constant stress formulation. The cross-section integrated beam element (Hughes-Liu beam in LS-DYNA) is used for the slab reinforcement. The mesh size for the main components of the floor system including the girders, joists, columns, ties, and their connections ranges from 10 to 15 mm. The mesh size of the concrete slab and its reinforcement increased to 50 mm.

The Winfrith concrete model (MAT085) and the elastic-plastic-thermal model (MAT04) in LS-DYNA are used for the concrete slab and steel components, respectively. The use of MAT04 in the software allows for consideration of temperature effect on the steel

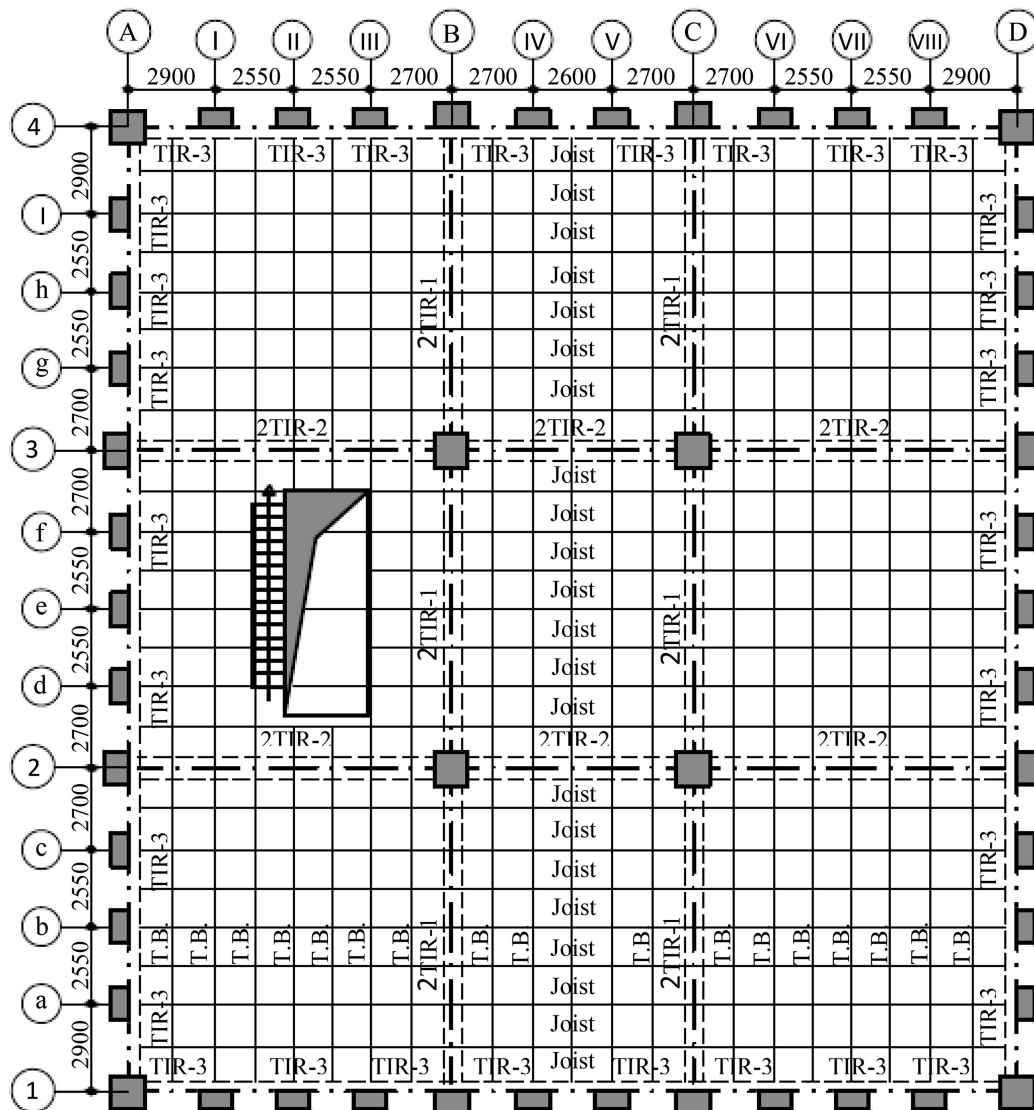


Figure 2. Structural plan view of the building.

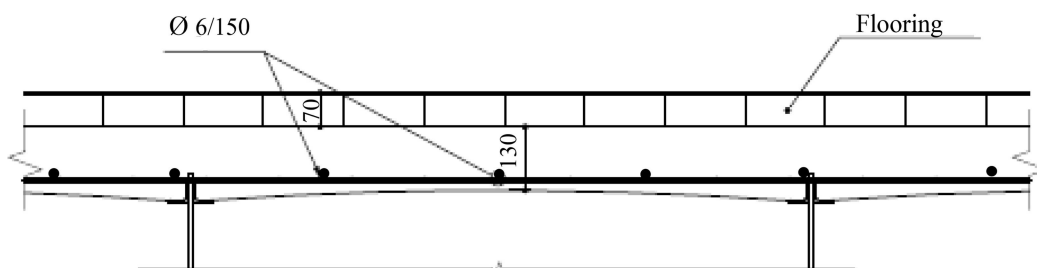


Figure 3. Details of concrete slab.

material properties (i.e., Young's modulus, Poisson's ratio, the coefficient of thermal expansion, yield stress, and plastic hardening modulus). Of the steel material properties, Young's modulus and yield stress are changed as a function of temperature and the other parameters are assumed constant. The effect of temperature on the material properties of the concrete

slab and its reinforcement is ignored. Based on the measured material properties of the coupon steel specimens and concrete cylinders, an ASTM A36 steel with a yield stress of 235 MPa and a C30 grade with a concrete compressive strength of 27.5 MPa are used for the steel and concrete materials, respectively. Given the lack of experimental data on the welding

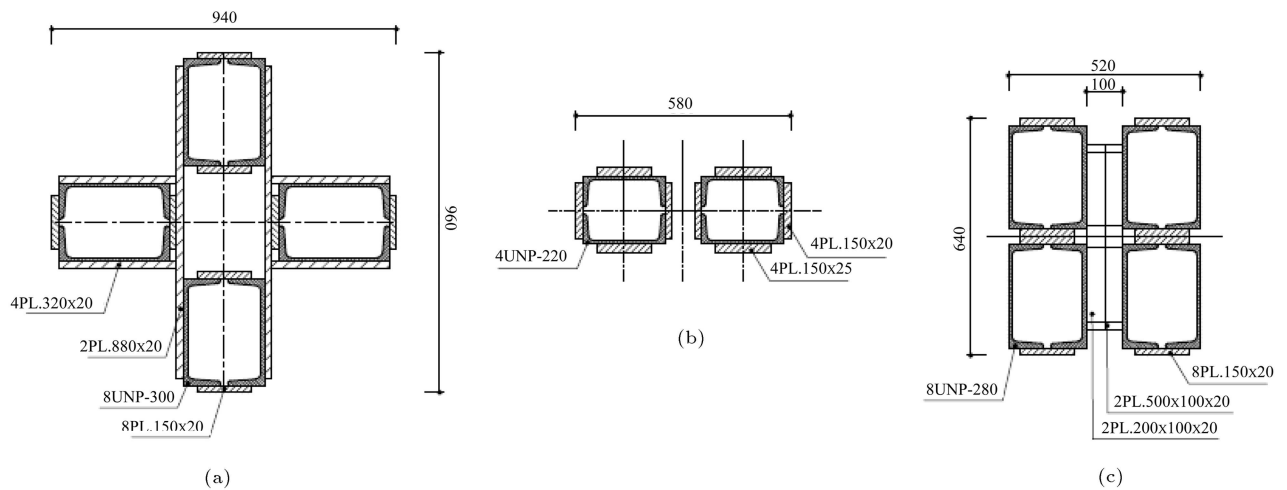


Figure 4. Cross-section of the columns.

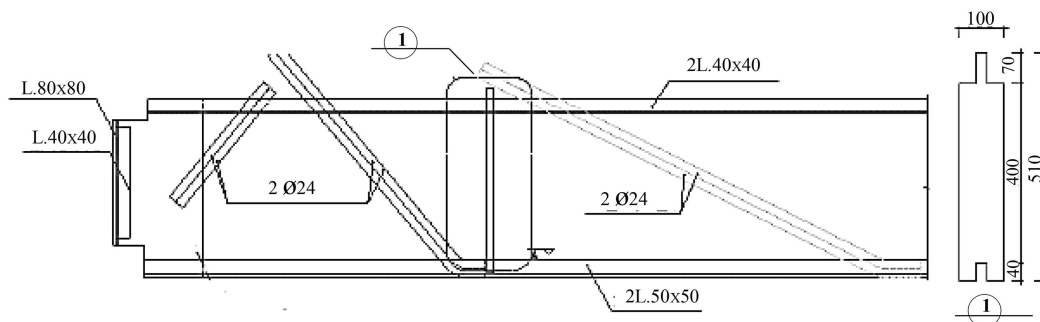


Figure 5. Floor joist.

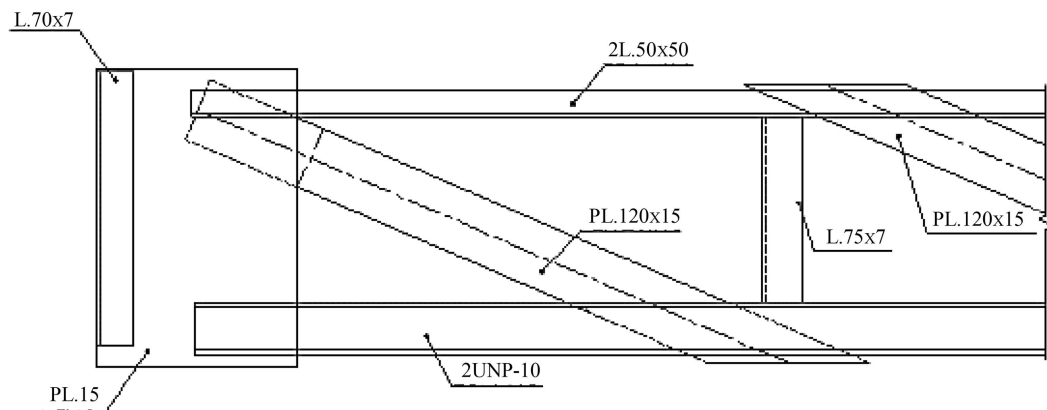


Figure 6. Floor girder connected to the corner column.

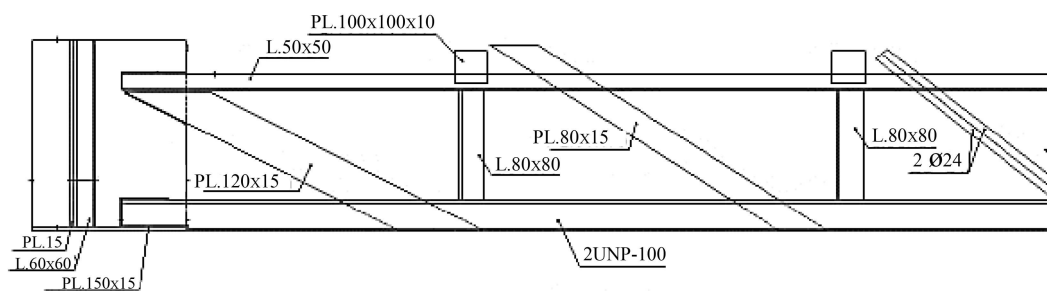


Figure 7. Floor girder connected to the perimeter column.

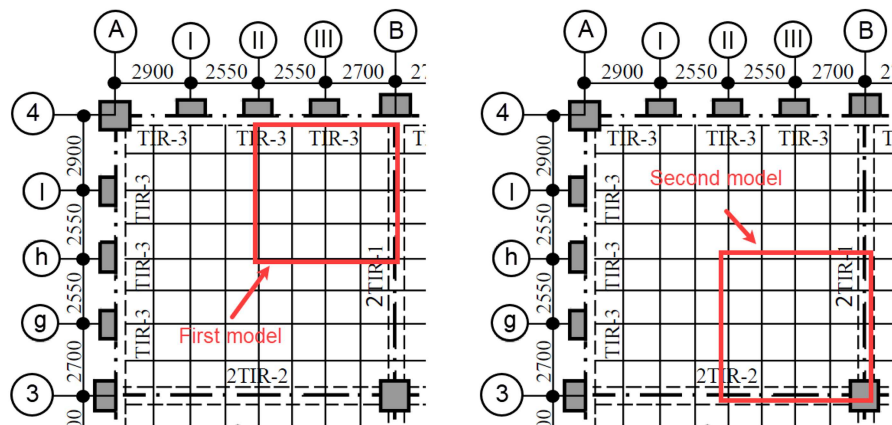


Figure 8. Modeled zones in LS-DYNA.

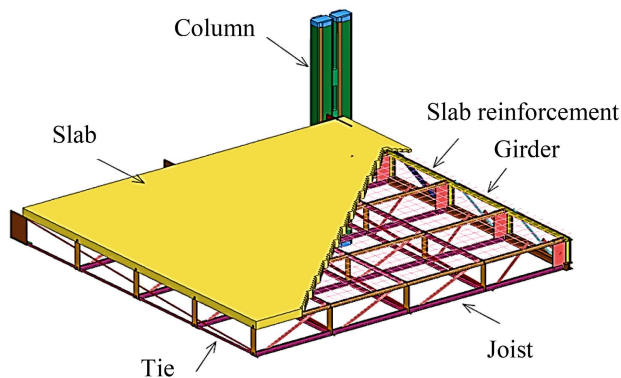


Figure 9. LS-DYNA model of a quarter of the floor panel.

material, the material properties of the welds are assumed equal to those of E60 electrode. The effect of temperature on the elasticity modulus is presented in Figure 12 [25].

The fracture of the steel and weld elements is considered using erosion strains (i.e., maximum principal strain) of 12% and 8% for the steel and weld elements, respectively. Two erosion strains are defined for the concrete slab: a compressive erosion strain (i.e., minimum principal strain) of -0.005 and a tensile erosion strain (i.e., maximum principal strain) of 0.002 .

Two gravity and thermal loads are applied to the structure. The gravity load is applied first and then, the girders, joists, ties, and columns are subjected to the thermal load. Due to the existence of some fireproof materials such as gypsum boards and light concrete around columns of the building and according to the results of a finite element analysis of the effect of fireproofing material on the temperature distribution among structural components, a 200°C difference between the temperatures applied to the beams and columns is considered.

4. Predicted and observed damages to structural components

Herein, the results of the nonlinear analysis of the LS-DYNA models are compared with the failure modes of the structural elements investigated during the site visits. Figure 13 presents the damage to the girder-to-column connection of the first model including the fracture of the gusset plate welds and the fracture of the channel section. According to Figure 13, the LS-DYNA predicted damage which matched the failures observed following the collapse of the structure.

Figure 14 shows the LS-DYNA predicted and observed damages to the steel girders of the second

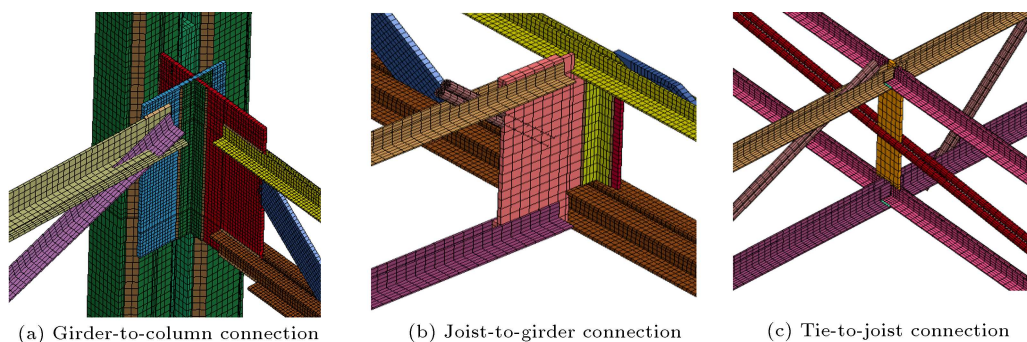


Figure 10. Various connections modeled in LS-DYNA.

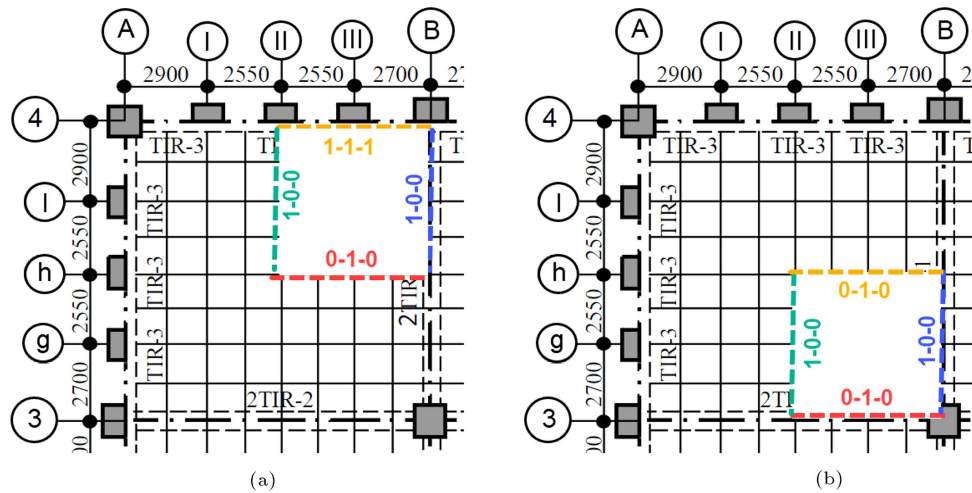


Figure 11. The boundary condition of the LS-DYNA models: (a) Model 1 and (b) Model 2.

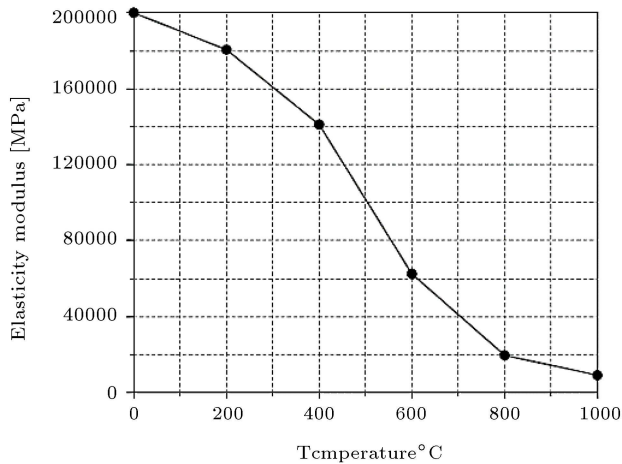


Figure 12. The effect of temperature on elastic modulus.

model. The top double angles of both predicted and observed girders experience excessive out-of-plane deformation and the red colored zone in the numerical model shows the yield part in the failed specimen. In addition, the fracture at the connection between the top angles and vertical strap is captured as well.

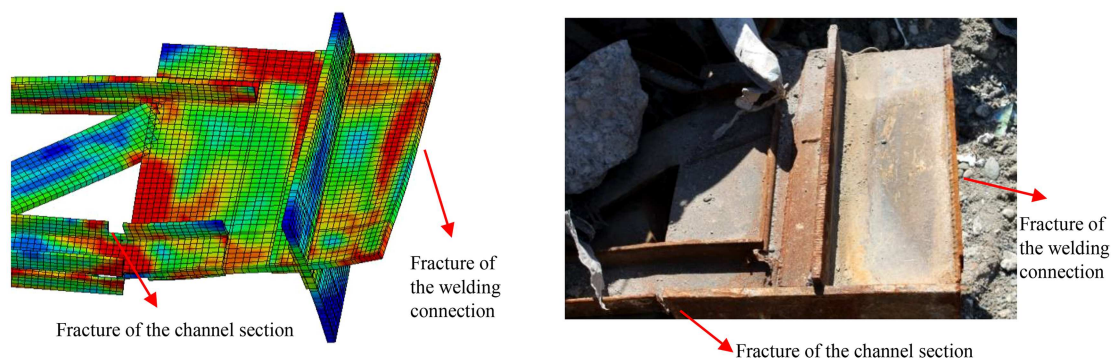


Figure 13. Failure at the connection between the girder and column.

5. Analysis of results

In this section, the local failure of each member of the Plasco building is investigated using the nonlinear analysis of the structure.

The deflection ratios of the steel girder to the vertical displacement of the panel at its mid-point at two stages of loading including full gravity and full gravity plus thermal loadings are presented in Figure 15. The deflection ratio is defined as the ratio of the vertical displacement at the mid-length of the girder or mid-point of the panel to the length of the beam or length of the panel. Figure 15 indicates that the deflection ratio of the girder (solid line in Figure 15(a)) ranges from 0% to 0.4% (0 to 1/250) as gravity load increases from 0% to 100%. As expected, the deflection ratio of the mid-point of the panel (dashed line in Figure 15(a)) is greater than its corresponding deflection of the girder at each level of the gravity load. Figure 14(b) indicates that the deflection ratio ranges from 0.4% (1/250) up to the large value of 8.2% (1/12) and from 0.6% (1/67) to 10% (1/10) for the girder and panel, respectively, which exceed the allowable deflection ratio of (1/20), as

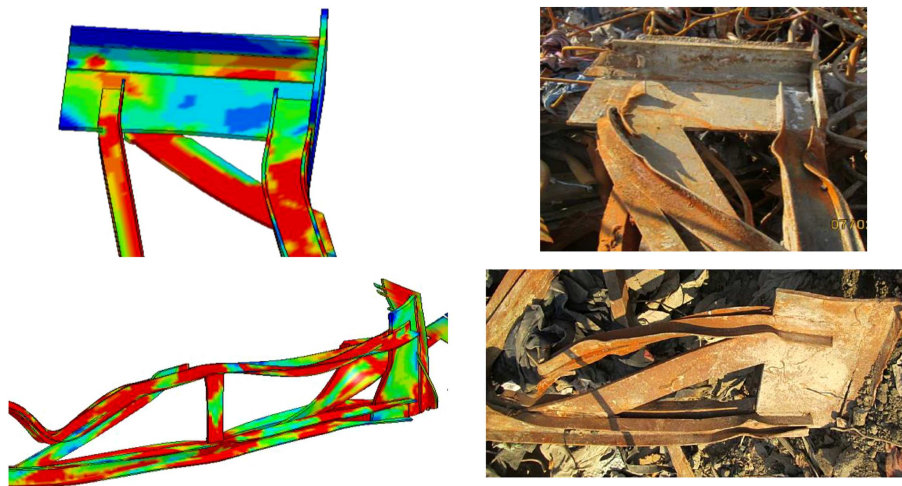


Figure 14. Deformed shape and buckling of the components of the girder.

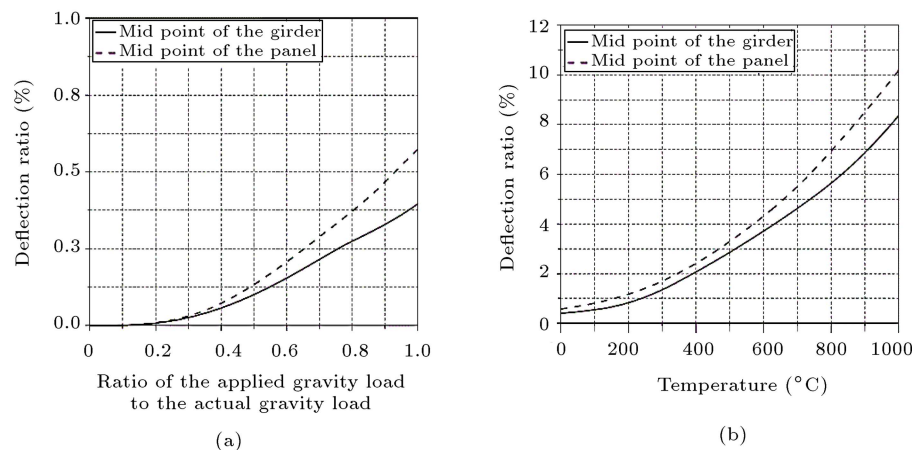


Figure 15. Beam and slab deflections due to gravity and thermal loadings: (a) Gravity loading and (b) thermal loading.

the temperature increases from 0 to 1000°C. Based on the part 20 of BS 476 [26], the deflection of beam and floor slab is limited to $(L/20)$ or when the deflection exceeds $(L/30)$, the rate of the deflection is limited to $(L^2/9000d)$ where L is the length span in mm and d is the distance from the structural section to the bottom of the design tension zone in mm.

5.1. RC slab

The LS-DYNA predicted crack pattern in the Reinforced Concrete (RC) slab at different stages of the gravity and thermal loadings is presented in Figure 16. The cracks are negligible at the end of gravity loading. As thermal loading is applied and increases, joists, which are designed to control the deflection of the slab, buckle and their load carrying capacity is lost. Therefore, the deflection of the RC slab becomes excessive and the cracks are propagated on the bottom face of the RC slab where it is connected to the joists and between two joists.

5.2. Tie beam

Figure 17 presents the Von-Mises stress contours of the tie beams at full gravity plus different thermal loadings. As Figure 17 indicates, there is yielding in some bars of the tie beams at the end of the gravity loading. As temperature is applied and increases up to 400°C, the bottom double angles experience an out-of-plane deformation since they are not constrained in the RC slab. The increment of out-of-plane deformation of double angles leads to fracture at the connection between the double angles and vertical straps at 800°C.

5.3. Joist

Joists play an important role in load carrying as they transfer load from slab to girder. Figure 18 shows that the joists have an elastic behavior except some local yield zones up to 600°C. As joists buckle and accordingly, the propagation of cracks at the RC slab occurs at the top of the joists, the slab cannot prevent the excessive buckling of the joists. At 800°C up to

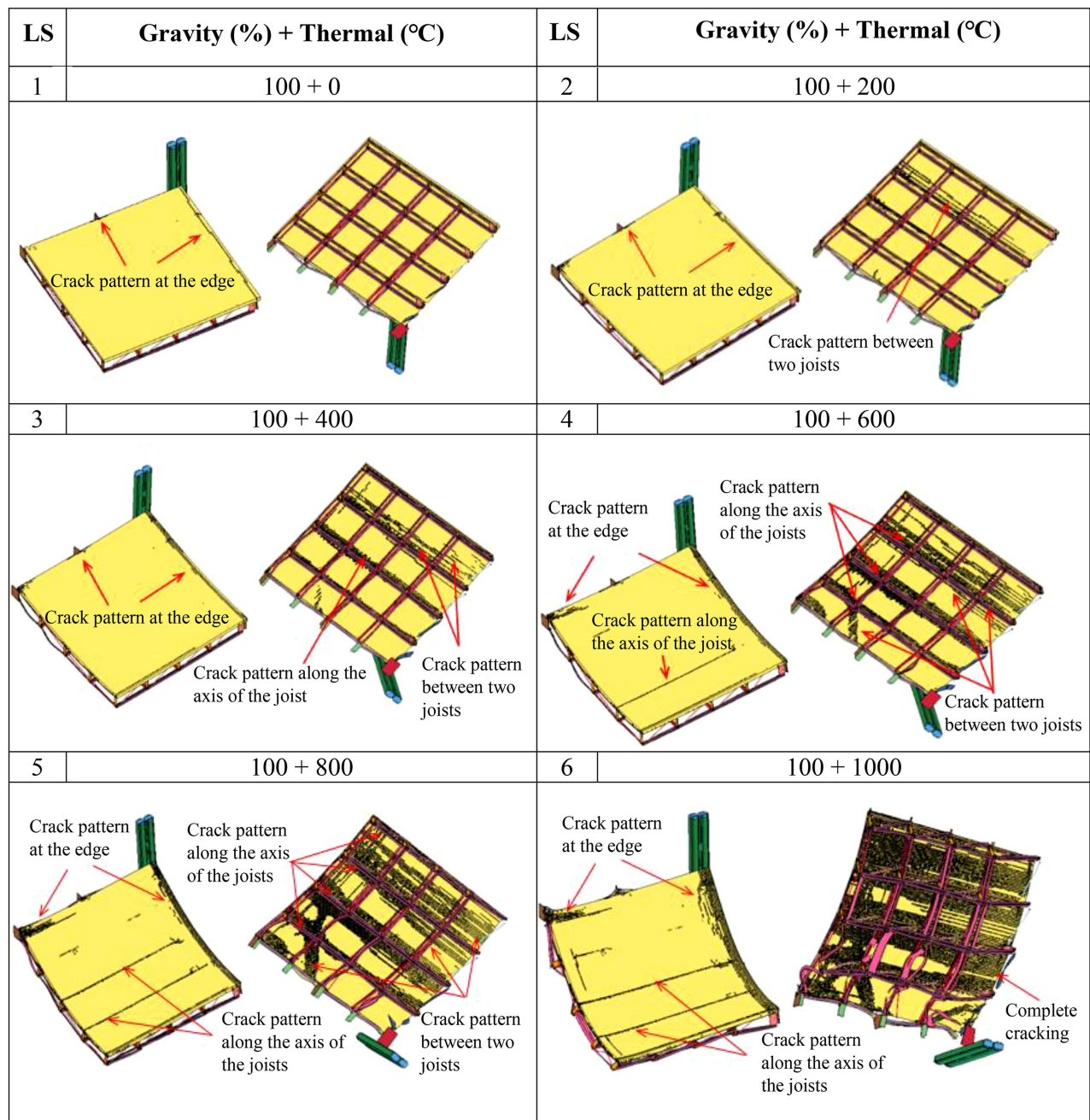


Figure 16. LS-DYNA predicted cracking of the RC slab due to gravity and thermal loadings.

1000°C, buckling of the joists, fracture of the tie beam-to-joist connection, and collapse of the RC slab cause fracture of the connection between bottom double angles and vertical strap and accordingly, the joist-to-girder connection is fractured, as well.

5.4. Edge girder

LS-DYNA prediction of stresses in the edge girder due to full gravity plus different thermal loadings is presented in Figure 19. The fracture of the connection between tie beam and edge girder causes the excessive out-of-plane buckling of the top angles of the edge

girder at 800°C. As temperature increases further (at 1000°C), buckling of the top angles and vertical strap cause the torsion of the diagonal angles, leading to the loss of girder capacity to carry loading.

5.5. Main girder

As thermal load is applied and increased, thermal elongation of joists causes compressive force at the top angles and the bottom channels of the girder. The compressive force leads to the out-of-plane deformation in the girder since the out-of-plane stiffness of the top angles and bottom channels is low to provide sufficient

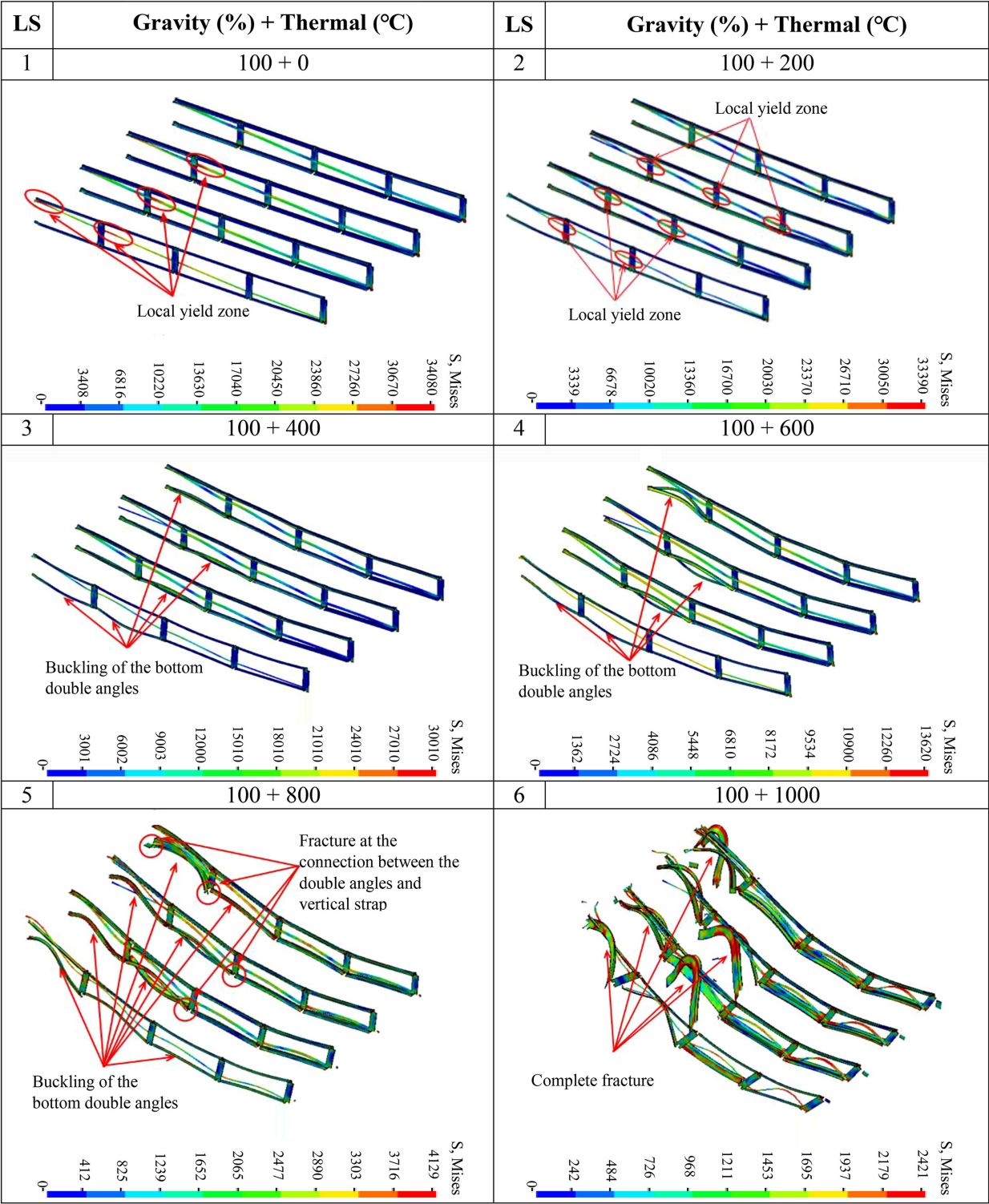


Figure 17. LS-DYNA predicted damage to the tie beams due to gravity and thermal loadings.

stiffness to the deformation. Furthermore, with the application of the thermal load, the girder length tends to increase and therefore, a compressive axial force is generated due to its end constraints and both the top angles and the bottom channels accordingly buckle.

Buckling of the top angles and bottom channels leads to their fracture, as seen in Figure 20.

5.6. Column

Von-Mises stress distribution in column due to gravity

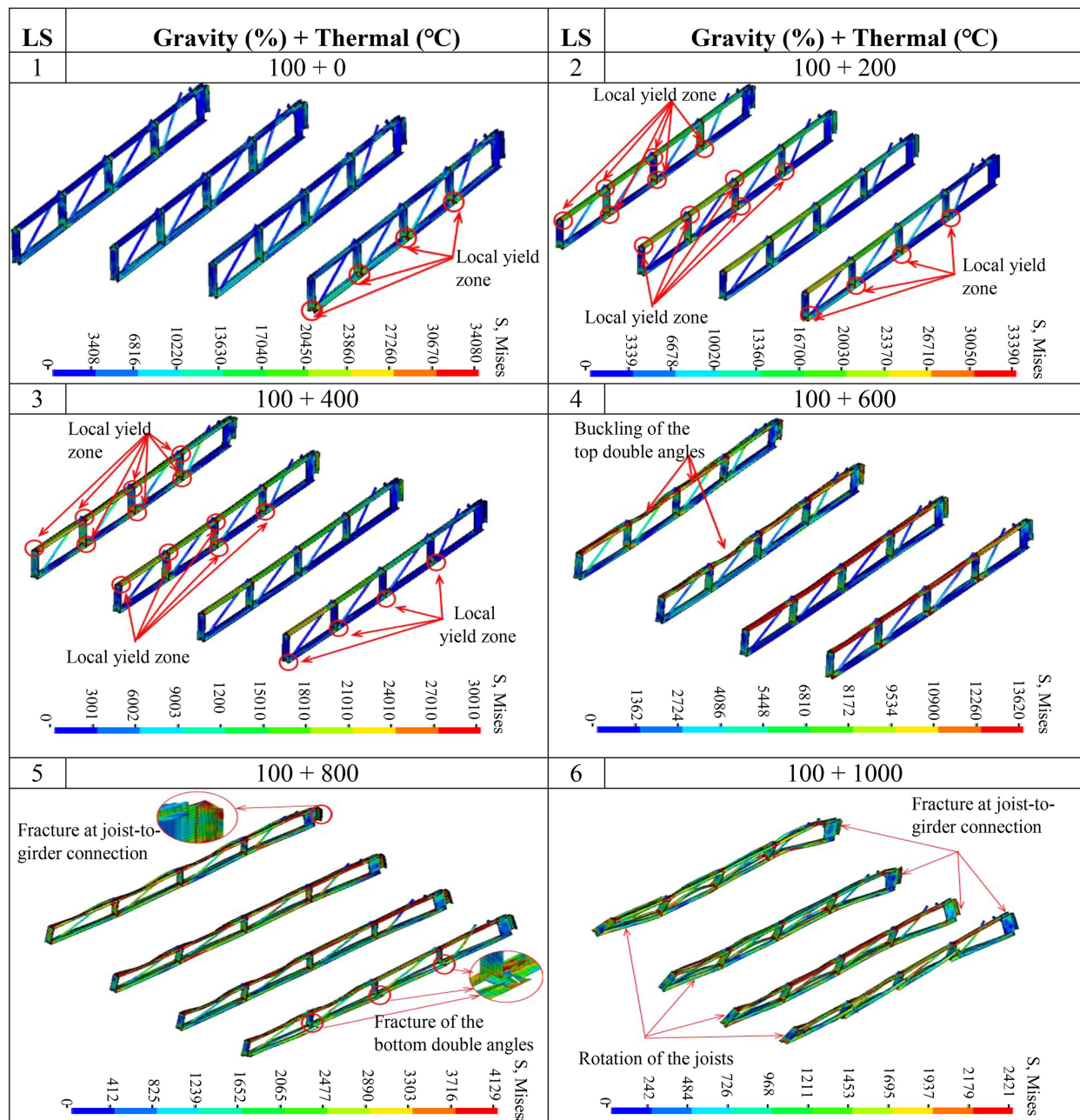


Figure 18. LS-DYNA predicted damage to the joists due to gravity and thermal loadings.

and thermal loadings is presented in Figure 21. There is no buckling or yielding in the column, as there is not a red colored zone in Figure 21. These results show the column have sufficient stiffness and strength to resist the gravity and thermal loadings without a considerable damage at the end of loading process.

6. Progressive collapse

In previous sections, the LS-DYNA prediction of the local failure of each member was discussed. Herein,

the main reason of fire-induced progressive collapse is discussed.

The behavior of a steel beam under fire is often governed by its flexural bending response at elevated temperatures. However, in the presence of axial restraint, the beam at large deflections behaves differently. Indeed, the effect of axial restraint at large deflection is not negligible and can cause a catenary action in the beam, which can become the main load-carrying mechanism. In catenary action, the beam will be mainly in tension and resist the bending moment due to applied vertical load by catenary force in the

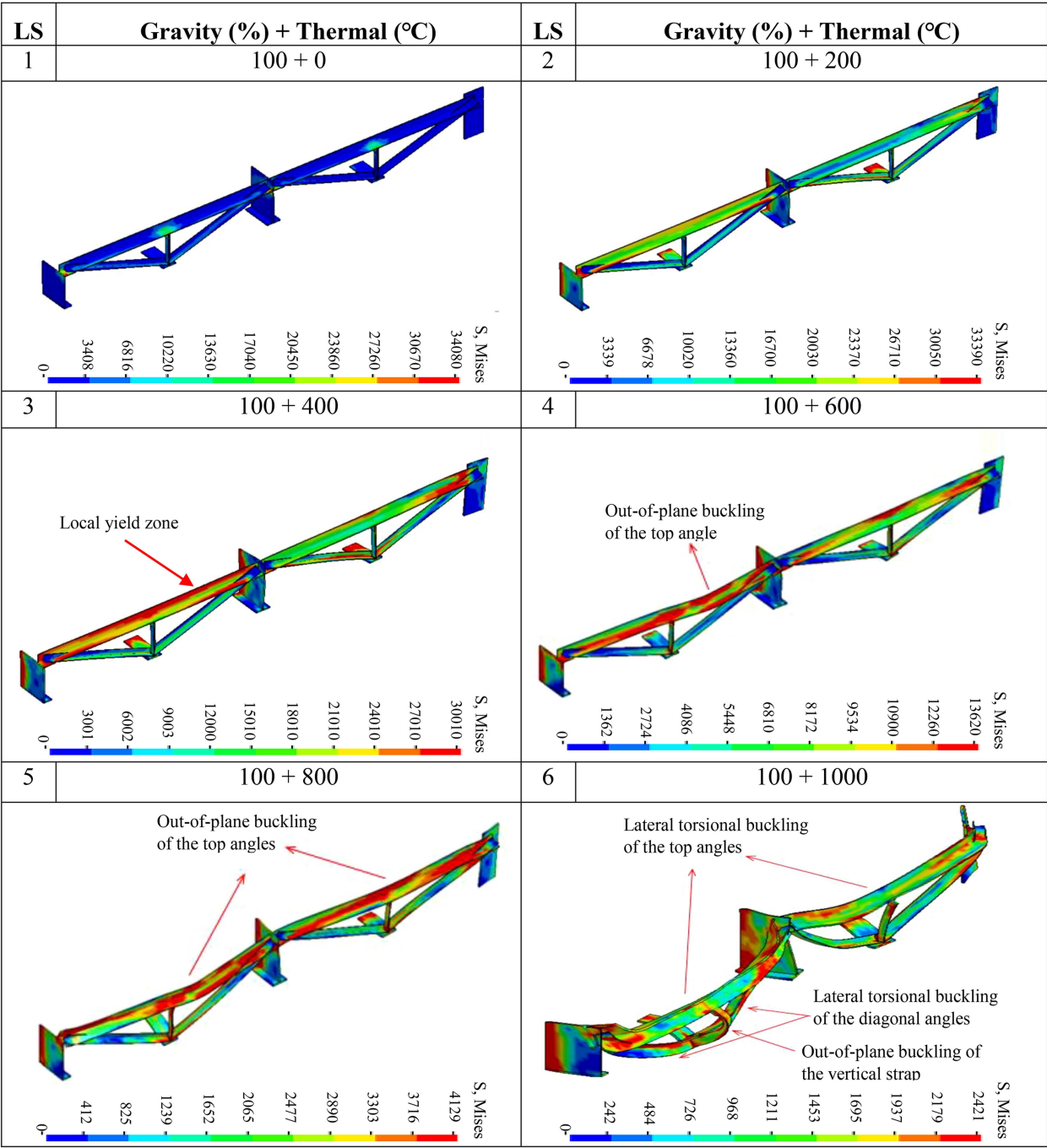


Figure 19. LS-DYNA predicted damage to the edge girder due to gravity and thermal loadings.

beam. The catenary force, however, is transferred to the end connections of the beam resulting in premature failure if they are not designed to resist this tension force.

The Plasco investigation indicates that the major source of rupture in the connections and its following progressive collapse of the structure resulted from catenary action in the connections. As Figure 22 shows, as thermal loading is applied (up to 110°C) in the presence of 100% gravity, the compressive axial force in the

bottom channels increases. As temperature increases further (above 110°C), the compressive force decreases due to catenary action in the beam and at nearly 700°C, the fracture of the bottom channels occurs. The top double angles follow the same trend, except that the initiation of the catenary action occurs at 200°C since they do not experience excessive buckling like the bottom channels. Figure 22 presents that the diagonal plates are less sensitive to the catenary action and it is more critical for horizontal members.

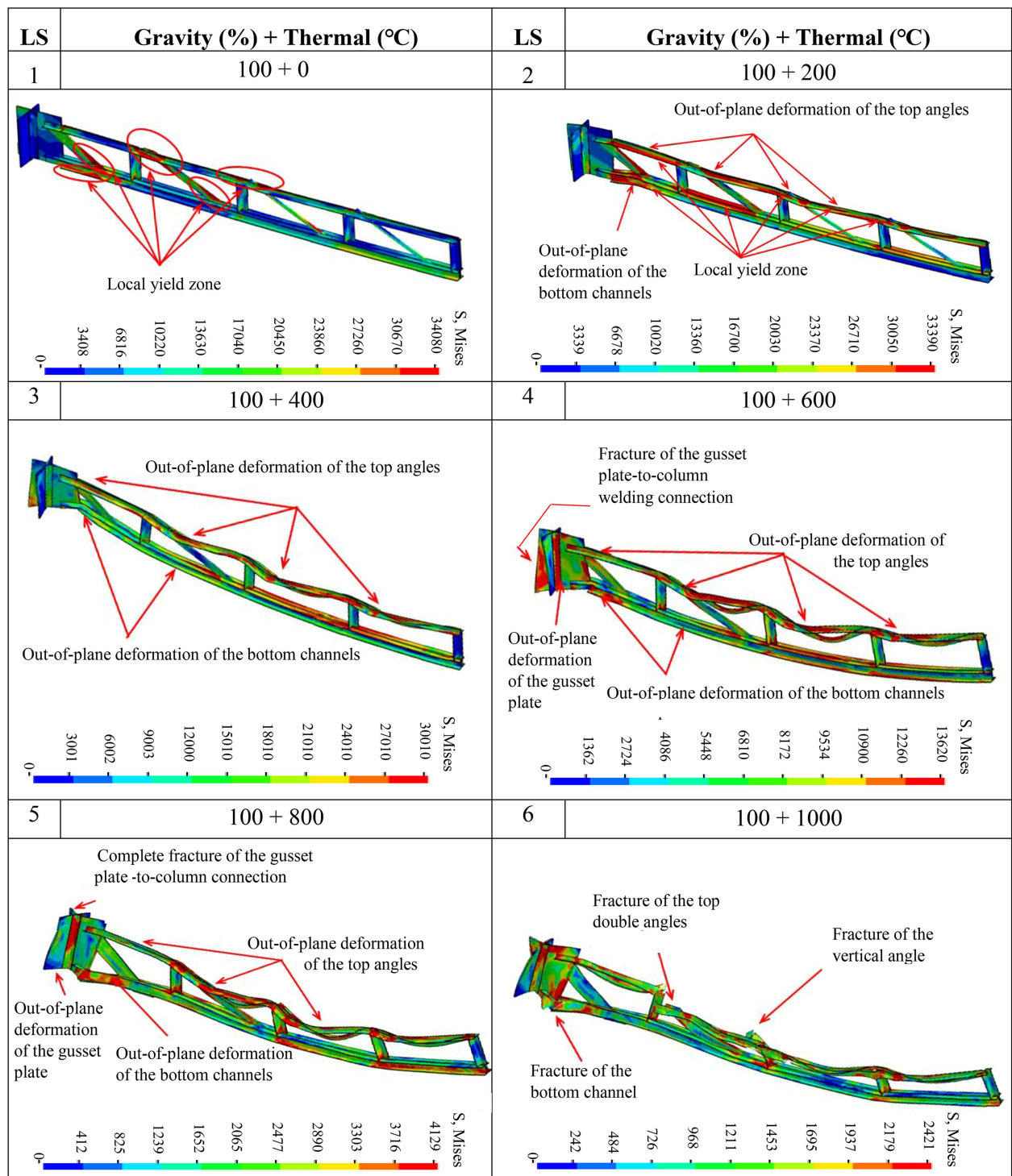


Figure 20. LS-DYNA predicted damage to the girder due to gravity and thermal loadings.

The tensile axial force in the gusset plate decreases when the thermal load is applied (up to 200°C). As a temperature increases (above 200°C), the compressive axial force in the gusset plate decreases due to catenary action and the gusset-to-column connection is fractured at 700°C mainly by two simultaneous mechanisms. The first mechanism is an out-of-plane deformation of

the bottom edge of the gusset plate due to thermal elongation of the joists and buckling of the bottom channel of the main girder, and the second mechanism is the catenary force transferred to the gusset from the main girder. Finally, the fracture of the connection between gusset and column causes the collapse of the whole structure.

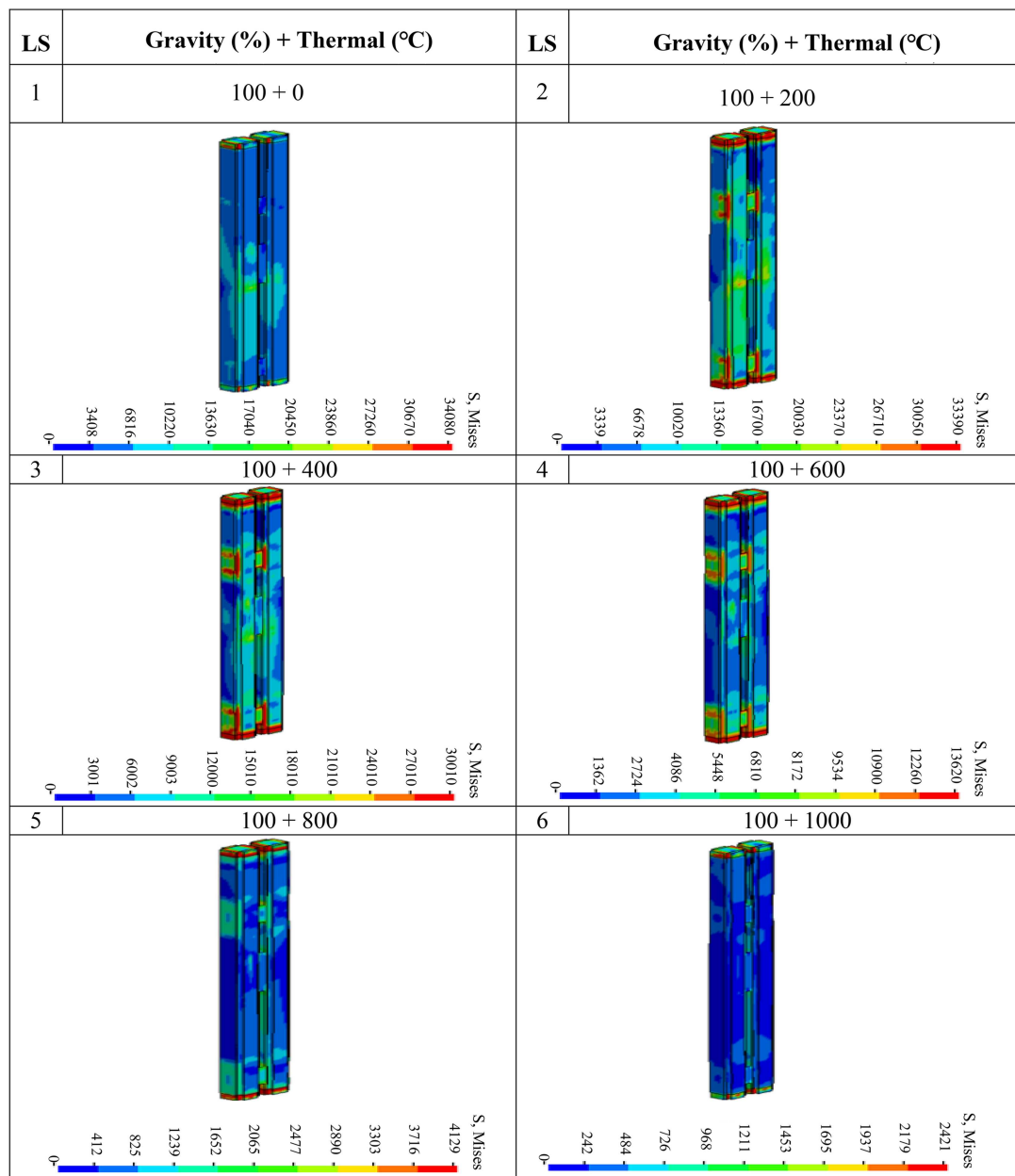


Figure 21. LS-DYNA predicted damage to the corner column due to gravity and thermal loadings.

A brief explanation of behavior of each member of the Plasco building at various stages of full gravity plus thermal loadings is provided in Table 1.

7. Design recommendations

The progressive collapse of the Plasco building due to failure of the girder-to-column connection was discussed in detail in previous sections. Therefore, a number of recommendations are made to prevent similar disasters in future constructions. The incidence of Plasco building revealed the importance of considering the interaction of flexural, shear, and catenary demands in designing structures under fire, which

is not assumed in any available regulation regarding fire safety. Up to now, the design of a steel beam under fire has been based on the flexural behavior of the beam according to general rules of structural fire design in EN1993-1-2 code [27]. However, the results of this research indicate when the beam is axially restrained in the presence of large deflection under fire, the connections experience catenary force at high temperatures. Since the connections are not typically designed for the interaction between other forces and catenary force, they fail and cause the collapse of the whole structure. Therefore, the inclusion of catenary force together with other typical demands in the design of structures in fire conditions, especially in structures

Table 1. Summary of the structural damage to all the members of the first model at various stages of the gravity and thermal loadings.

LS	1	2	3	4	5	6
$G + T^*$	100	100 + 200	100 + 400	100 + 600	100 + 800	100 + 1000
RC slab	Negligible cracking at the top face edge	Cracking at the bottom face between two joists	cracking at the bottom face between two joists and along the axis of the joist	Increase in cracking at the bottom face between two joists and along the axis of the joist	Increase in cracking at the bottom face between two joists and along the axis of the joist	Complete cracking of the bottom edge
Tie beam	Local yield at the double bars-to-vertical strap connections	Local yield at the double bars-to-vertical strap connections	Buckling of the bottom double angles	Increase in Buckling of the bottom double angles	Increase in Buckling of the bottom double angles and fracture at the connection between the double angles and vertical strap	Complete fracture
Joist	Local yield at the vertical strap-to-bottom double angles connections	Local yield at the vertical strap-to-bottom and top double angles connections	Local yield at the vertical strap-to-bottom and top double angles connection	Buckling of the top double angles	Fracture at the joist-to-girder connection and bottom double angles	Rotation of the joists due to the collapse of the slab
Edge girder	Elastic behavior	Elastic behavior	Local yield at one of the top angles	Buckling of the one of the top angles	Buckling of the both of the top angles	Buckling of the vertical strap causing the torsion of the diagonal angles
Girder	Local yield at different parts	Increase in local yield and out-of-plane deformation of the top double angles and bottom double channels	Increase in Out-of-plane deformation of the top double angles and bottom double channels	Starting out-of-plane deformation of the bottom gusset plate and fracture of the gusset plate-to-column connection and increase in out-of-plane deformation of the top double angles and bottom double channels	Complete fracture of the gusset plate-to-column connection	Fracture of the top double angles, bottom channel, and vertical angle-to-bottom channel connection
Column	Elastic behavior	Elastic behavior	Elastic behavior	Elastic behavior	Elastic behavior	Elastic behavior
Connection	Elastic behavior	Elastic behavior	Elastic behavior	Starting out-of-plane deformation of the bottom gusset plate and fracture of the gusset plate-to-column connection	Increase in out-of-plane deformation of the bottom gusset plate and complete fracture of the gusset plate-to-column connection	Complete fracture

 $G + T^* = \text{Gravity (\%)} + \text{Thermal (}^\circ\text{C)}$

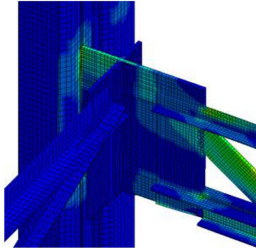
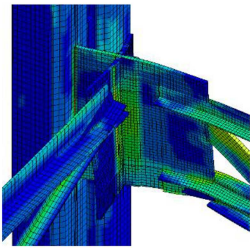
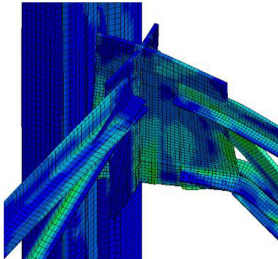
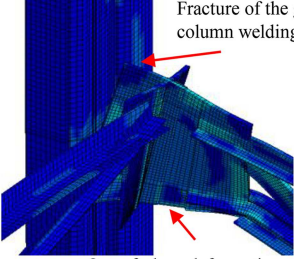
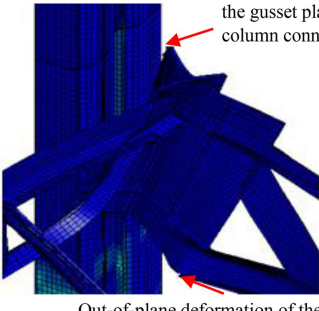
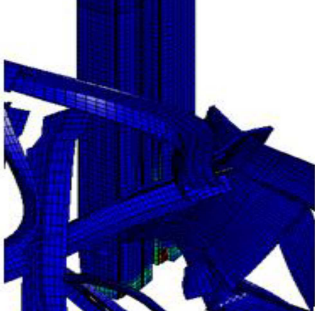
LS	Gravity (%) + Thermal (°C)	LS	Gravity (%) + Thermal (°C)
1	100 + 0	2	100 + 200
			
3	100 + 400	4	100 + 600
			
5	100 + 800	6	100 + 1000
			

Figure 22. LS-DYNA predicted damage to the girder-to-column connection due to gravity and thermal loadings.

with opening web in which elements are prone to damage due to catenary force, needs to be considered in design standards and guidelines.

Providing a continuous load path in elements and connections is another important provision that needs to be considered in the design of structures. As explained in Section 2.4. of AISC 358 [28], continuity and stiffener plates for columns in rigid connections should be provided to ensure a continuous load path from beams to columns. Utilizing continuity plates prevents any local failure in column (e.g., crippling, yielding, and sideways and compression buckling in column web and bending in column flanges) and makes the stress distribution at the beam-to-column connection uniform. In the Plasco building, continuity plates in the columns were not considered along the gusset plate, although the connections were rigid. The flexural force in the girder along with the catenary force led to the considerable bending of the gusset plate and rotation at a beam-to-column connection in the absence of continuity plates, which could prevent

out-of-plane deformation of the column flange. This confirms that the absence of continuity plate has a significant role in the structural failure of the buildings.

8. Summary and conclusions

In this paper, a quarter of the most critical panel at the eleventh floor of the Plasco building was simulated using the LS-DYNA program. To overcome computational cost and reduce the time of analysis, some simplifying assumptions not affecting the overall results were used in analysis. Results of the nonlinear analysis confirmed the failure mechanism of the structure inferred from site investigations. Based on the analysis results, the failure of the main girder-to-column connections was associated to the out-of-plane deformation of the gusset plate and catenary action in the girder. The connection rupture and collapse of the girders led to overall instability and collapse of the whole structure.

As an important lesson from this tragic incident,

the effect of catenary action together with all routine flexural and shear demands must be considered in the design of structural connections of the steel structures in the fire condition. Furthermore, the use of continuity plates in columns is essential to providing a continuous load path in structure and preventing any local failure of the connection.

Acknowledgment

This investigation would not have been possible without the support of the many organizations and people involved in this event. The authors gratefully acknowledge the contribution to their work made by a national committee appointed for this task after the Plasco incident. This paper is dedicated to the memory of the 16 hero firefighters who were the heart-wrenching sacrifice of the faithful in this incident.

References

1. Fisher, J., "B structural steel and steel connections", *World Trade Center Building Performance study*, Appendix B, Federal Emergency Management Agency, FEMA 403 (2002).
2. Powers, W.R., *Report of Fire at One New York Plaza*, New York Board Underwriters, **85** (1970).
3. Gosselin, G.C. and Mawhinney, J.R. "A report on the alexis nihon office complex fire", National Research Council Canada, Internal Report No. 531 (1987).
4. Rahnavard, R., Siahpolo, N., Naghavi, M., et al. "Analytical study of common rigid steel connections under the effect of heat", *Advances in Civil Engineering*, **2014**, Article ID 692323, 10 pages (2014). <https://doi.org/10.1155/2014/692323>
5. Wald, F., Da Silva, L.S., Moore, D.B., et al. "Experimental behaviour of a steel structure under natural fire", *Fire Safety Journal*, **41**(7), pp. 509–522 (2006).
6. Eslami, M., Rezaeian, A., and Kodur, V. "Behavior of steel column-trees under fire conditions", *J. Struct. Eng.*, **144**(9), p. 04018135 (2018).
7. Sarraj, M., Burgess, I.W., Davison, J.B., et al. "Finite element modelling of steel fin plate connections in fire", *Fire Safety Journal*, **42**(6–7), pp. 408–415 (2007).
8. Wald, F.R., Strejček, M.I., and Tichá, A.L. "On bolted connection with intumescent Coatings", *Proc. 4th Int. Workshop Structural in Fire, Aveiro, Portugal*, pp. 371–22 (2006).
9. Al-Jabri, K.S., Seibi, A., and Karrech, A. "Modeling of un-stiffened flush endplate bolted connections in fire", *J. Constr. Steel Res.*, **62**, pp.151–159 (2006).
10. Al-Jabri, K.S., Burgess, I.W., Lennon, T., et al. "Moment-rotation temperature curves for semi-rigid joints", *J. Constr. Steel Res.*, **61**, pp. 281–303 (2005).
11. Daryan, A.S. and Yahyai, M. "Modeling of bolted angle connections in fire", *Fire Safety Journal*, **44**(7), pp. 976–988 (2009).
12. Daryan, A.S. "A study on behavior of connections in fire", Doctoral Dissertation, MS thesis, K.N. Toosi University, Tehran, Iran (2006).
13. Daryan, A.S. and Yahyai, M. "Behavior of bolted top-seat angle connections in fire", *J. Constr. Steel Res.*, **65**(3), pp. 531–541 (2009).
14. Zhu, M.C. and Li, G.Q. "Behavior of beam-to-column welded connections in steel structures after fire", *Procedia Engineering*, **210**, pp. 551–556 (2017).
15. Zhang, G., Zhu, M.C., Kodur, V., et al. "Behavior of welded connections after exposure to elevated temperature", *J. Constr. Steel Res.*, **130**, pp. 88–95 (2017).
16. Guo, Z. and Huang, S.S. "Behavior of restrained steel beam with reduced beam section exposed to fire", *J. Constr. Steel Res.*, **122**, pp. 434–444 (2016).
17. Seif, M.S., Main, J.A., and Sadek, F.H. "Behavior of structural steel moment connections under fire loading", *Proc. Annual Stability Conf., Structural Stability Research Council* (2015).
18. Fletcher, I.A., Welch, S., Torero, J.L., et al. "Behaviour of concrete structures in fire", *Thermal Science*, **11**(2), pp. 37–52 (2007).
19. Jiang, J. and Usmani, A. "Modeling of steel frame structures in fire using OpenSees", *Computers & Structures*, **118**, pp. 90–99 (2013).
20. Kotsovinos, P. and Usmani, A. "The World Trade Center 9/11 disaster and progressive collapse of tall buildings", *Fire Technology*, **49**(3), pp. 741–765 (2013).
21. Lange, D., Röben, C., and Usmani, A. "Tall building collapse mechanisms initiated by fire: mechanisms and design methodology", *Engineering Structures*, **36**, pp. 90–103 (2012).
22. Ahmadi, M.T., Aghakouchak, A.A., Mirghaderi, R., et al. "Collapse of the 16-story Plasco building in Tehran due to fire", *Fire Technology*, **56**(2), pp. 769–799 (2020).
23. LS-DYNA "Keyword user's manual Volume I", Version 971 R6.0.0, Livermore Software Technology Corporation (LSTC), Livermore, CA, USA (2012).
24. LS-DYNA "Keyword user's manual Volume II", Version 971 R6.0.0, Livermore Software Technology Corporation (LSTC), Livermore, CA, USA (2012).
25. Astaneh-Asl, A., Noble, C.R., Son, J., et al. "Fire protection of steel bridges and the case of the MacArthur maze fire collapse", In *TCLÉE 2009, Lifeline Earthquake Engineering in a Multihazard Environment*, pp. 1–12 (2009).
26. British Standards Institution, *Fire Tests on Building Materials and Structures* (1987).
27. European Committee for Standardization, *General Rules-Structural Fire Design, EN1993-1-2*, Eurocode 3, Brussels (2005).

28. American Institute of Steel Construction “Prequalified connections for special and intermediate steel moment frames for seismic applications including supplement no. 1”, ANSI/AISC 358-16, American Institute of Steel Construction, Inc., Chicago, IL (2016).

Biographies

Siamak Epackachi is an Assistant Professor at the Department of Civil and Environmental Engineering of Amirkabir University of Technology (Tehran Polytechnic). He also serves as the Head of Iranian Society of Steel Structures. He has received his PhD from University at Buffalo in 2014. His teaching experience includes graduate and undergraduate courses at several prominent institutes including University at Buffalo, Sharif University of Technology, and Amirkabir Uni-

versity of Technology. His main research interests include the behavior of composite structures, and hybrid modeling and testing.

Seyed Rasoul Mirghaderi is a Professor at School of Civil Engineering, College of Engineering, University of Tehran. He currently serves as the Head of the Iranian National Building Code (Part 10). He has received his PhD from Purdue University in 1982. His main research interests include the steel design of structures, stability analysis, and composite design.

Pariya Aghelizadeh is a graduate student at the Department of Civil and Environmental Engineering of Amirkabir University of Technology (Tehran Polytechnic). His research interests include experimental studies and finite element analysis of structures.